

# **GeoStudio Example File Parameterizing the Soft Soil Model**

To see the latest GeoStudio learning content, visit <u>Seequent Learning Centre</u> and search the catalogue for "GeoStudio".

## Introduction

This example demonstrates how to parameterize the Soft Soil Cap constitutive model from laboratory data. The parameters are then used in numerical simulations of the laboratory tests and the simulated results are compared with the measured data and analytical solutions.

#### **Formulation**

A brief overview of the soft soil cap model is provided as a prerequisite to the parameterizing procedure. Details of the formulation are presented in the reference book (Seequent ULC, 2024). Note the following in reference to Figure 1:

- 1. The stress-strain response is assumed linear in  $\varepsilon_v \ln(p + c \cot \varphi)$  space.
- 2. Isotropic compression of an overconsolidated soil produces a stress-strain response that tracks along the overconsolidation line, which has a slope  $\kappa^*$ .
- 3. Continued isotropic compression causes the stress path to intersect the yield surface  $(p_p)$ , at which point the stress-strain path tracks along the normal compression line, which has a slope  $\lambda^*$ . The size of the elliptical yield surface which encloses the purely elastic zone expands to pass through the current stress state.
- 4. Unloading causes the stress path to track inside the yield locus and the stress-strain path to track along the unloading-reloading line. Reloading to the expanded yield locus will once again cause the soil to yield.

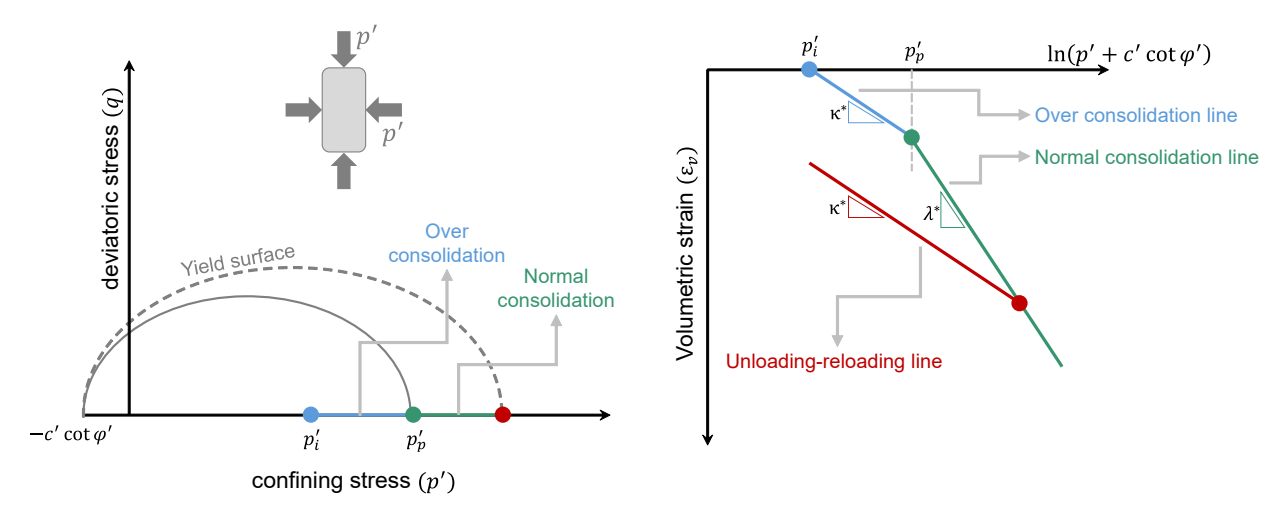


Figure 1. Soft Soil Cap model: response to isotropic compression.

Note the following in reference to Figure 2:

- 1. The deviatoric loading condition occurs when the major and minor principal effective stresses are not equal.
- 2. The stress path reaches the elliptical yield surface at a point away from horizontal axis.
- 3. In a  $\varepsilon_v \ln \left( p' + c' \cot \varphi' \right)$  space, the overconsolidation and unloading-reloading phases can still be considered as a line with the slope of  $\kappa^*$ ; however, the normal consolidation phase is not necessarily a straight line for a general anisotropic loading condition.



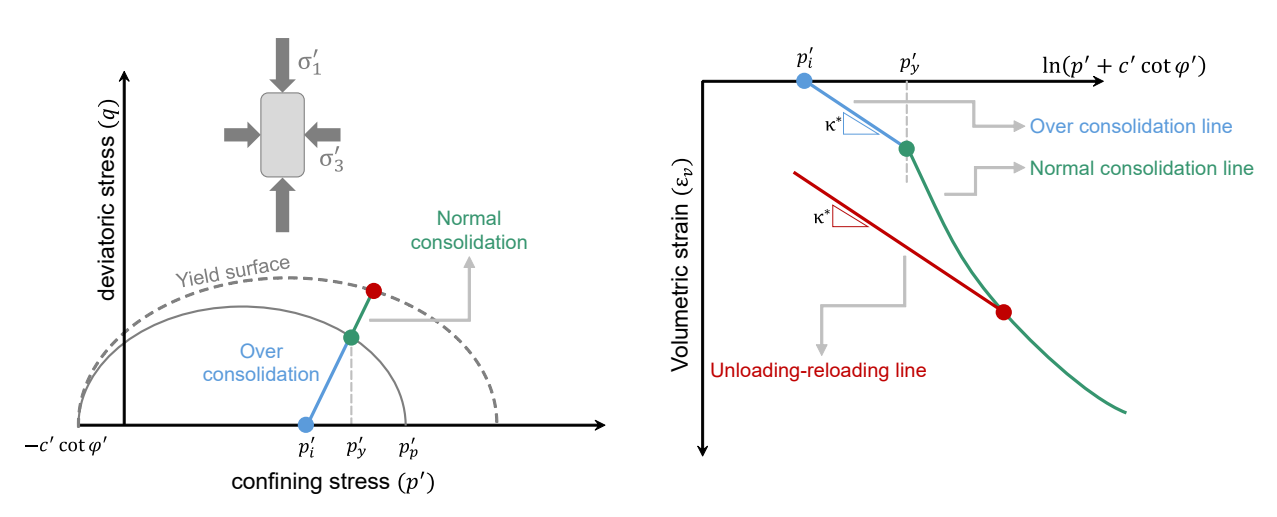


Figure 2. Soft Soil Cap model: response to a deviatoric loading condition.

Note the following in reference to Figure 3:

- 1. The Mohr-Coulomb failure criterion is assumed in the Soft Soil model.
- 2. The slope of the failure line can be expressed in terms of the effective friction angle in the Mohr-Coulomb failure criterion.
- 3. The yield surface is an ellipse in which the peak points pass through a straight line with a slope of M. This slope can be expressed in terms of the other model constants (i.e.,  $\lambda^*$ ,  $\kappa^*$ ,  $\kappa^{NC}$  and  $\mu_s$ ).
- 4. The over-consolidation ratio is the ratio between the maximum isotropic stress experienced by the sample and the current isotropic stress of the sample.
- 5. For a stress state inside the yield surface, the stress-strain response is elastic, and the compliance matrix is diagonal.
- 6. After reaching the yield surface and as it expands, the sample response becomes elastic-plastic and non-diagonal coupled components appear in compliance matrix. Incremental strains in this condition are the summation of elastic and plastic strains and so the current stress ratio plays a key role in the sample response.

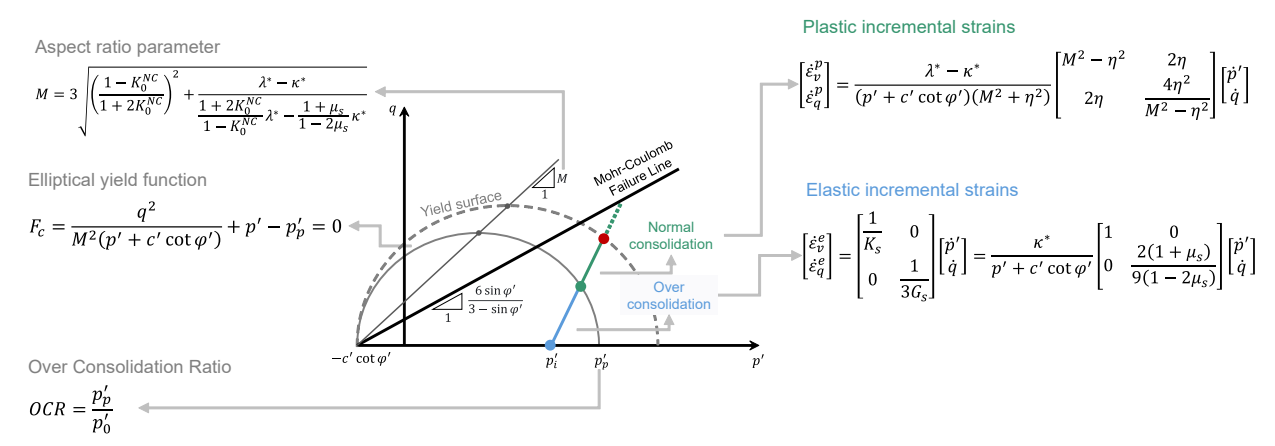


Figure 3. Soft Soil model: key ingredients of the formulation.

Table 1 summarizes the parameters of the Soft Soil model:

Table 1. Parameters for the Soft Soil model

Parameter	Symbol
Effective friction angle	$arphi^{'}$
Effective cohesion	c <sup>'</sup>
Slope of normal compression line in the $\varepsilon_{v}$ - $\ln (p' + c'\cot \varphi')$ space	λ*
Slope of the unloading-reloading line in the $\varepsilon_{v}$ - $\ln (p^{'} + c^{'}\cot \varphi^{'})$ space	κ*
The coefficient of earth pressure for the normally compressed state	$K_{0}^{NC}$
Poisson's ratio	$\mu_s$
Over consolidation ratio	OCR
Initial void ratio ( $e = v - 1$ )	e

## **Parameterization Procedure**

Figure 4 provides a conceptual workflow for the procedure. The parameterization procedure is premised on availability of drained triaxial test results. The parameterization procedure produces the constants for a specific constitutive model. These constants are then used as inputs for the model used in a numerical simulation. Finally, the parameterization is verified by comparing the simulated and measured results.

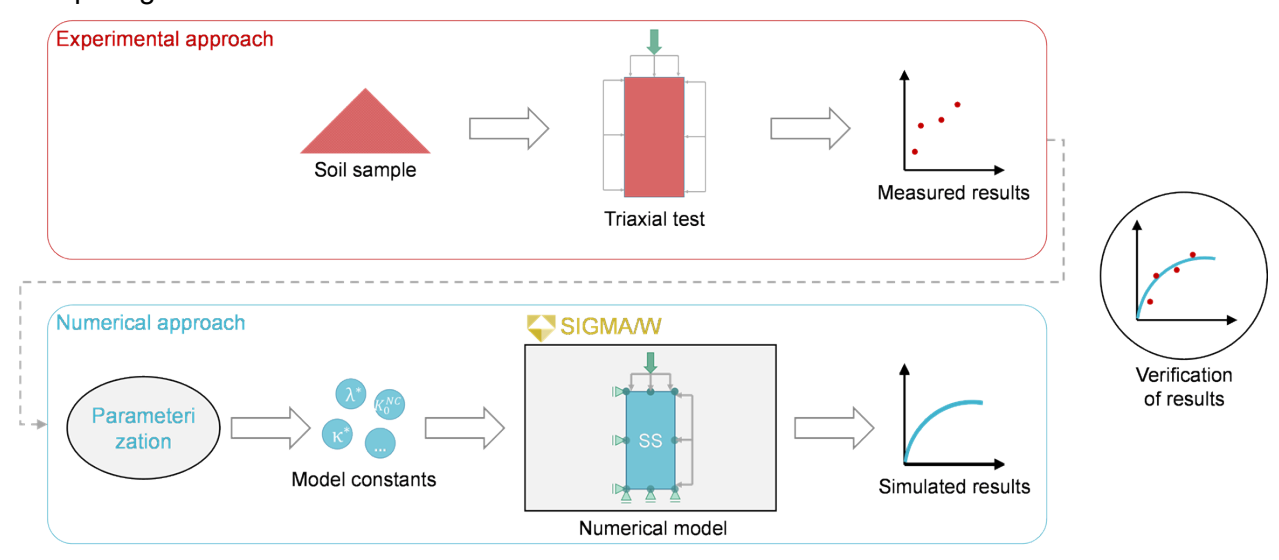


Figure 4. Conceptual workflow of the parameterization procedure.

## Step 1

The first step is to determine the slope and the y-intercept of the Mohr-Coulomb failure line and subsequently the effective friction angle and the effective cohesion of the soil (Figure 5). Since stress paths of samples with different initial confining stresses eventually tend to the failure line, the Mohr-Coulomb failure line is a straight line that passes through failure points. Let us call the slope of this line as  $^{M_c}$  and its y-intercept as  $^{q_c}$ . These two constants can be calculated using the method of least squares:



$$\begin{split} M_c &= \frac{n\sum q_f p_f^{'} - \sum q_f \sum p_f^{'}}{n\sum (p_f^{'})^2 - \left[\sum p_f^{'}\right]^2} \\ q_c &= \frac{\sum (p_f^{'})^2 \sum q_f - \sum q_f p_f^{'} \sum p_f^{'}}{n\sum (p_f^{'})^2 - \left[\sum p_f^{'}\right]^2} \end{split}$$
 Equation 2

The effective friction angle  $\varphi$  is the angle of the failure line relative to the horizontal axis in  $\tau$ - $\sigma$  space and the cohesion is the y-intercept of this failure line. As a result,  $\varphi$  and c can be calculated from  $^{M}{}_{c}$  and  $^{b}{}_{c}$ .

$$\varphi' = \sin^{-1} \frac{3M_c}{6 + M_c}$$
 Equation 3

$$c' = \frac{q_c}{M_c \cot \varphi}$$
 Equation 4

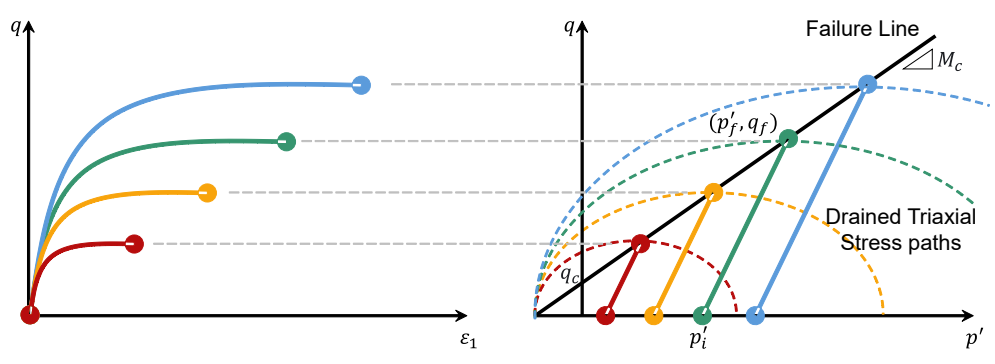


Figure 5. Determining the strength properties. Step 2

The second step is to determine the effective Poisson's ratio  $\mu_s$  (Figure 6). Poisson's ratio is defined as the ratio of the change in the element's radial strain to the change in its axial strain, in a drained test. Poisson's ratio is determined from the elastic (overconsolidated) response and its value is assumed to remain constant during loading. Consequently, in a drained triaxial test, the method of least squares can be applied on the purely elastic part of the curve in axial strain-radial strain space to estimate the value of the effective Poisson's ratio.

$$\mu_{s} = -\frac{\sum \varepsilon_{1} \varepsilon_{3}}{\sum {\varepsilon_{1}}^{2}}$$
 Equation 5



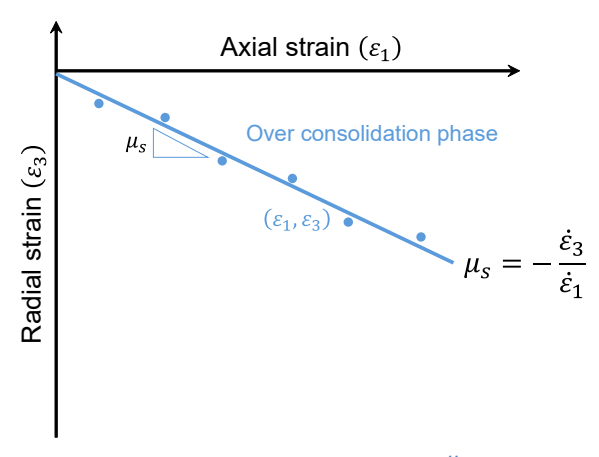


Figure 6. Determining Poisson's ratio  $\mu_{s}$ .

#### Step 3

The third step is to determine the slope of the overconsolidation line  $\kappa^*$  (Figure 7). The trends of the measured values of p' and  $\varepsilon_v$  in the overconsolidated portions of the graph can be fit by a straight line. The slope and the y-intercept of this line can be calculated directly using the method of least squares (blue line in Figure 7 and Equation 6 and Equation 7). An alternative method for estimating the constant  $\kappa^*$  is to use the corresponding parameters measured during an unloading-reloading loop (red line in Figure 7 and Equation 9 and Equation 10). For a normally consolidated soil, this unloading-reloading process is required for estimating the constant  $\kappa^*$ . The method of least square can again be used to calculate the slope and the y-intercept of this straight line.

$$\kappa^* = \frac{n\sum \varepsilon_{v,oc} x_{oc} - \sum \varepsilon_{v,oc} \sum x_{oc}}{n\sum x_{oc}^2 - \left[\sum x_{oc}\right]^2}$$
 Equation 6

$$\varepsilon_{v,oc}^{0} = \frac{\sum \varepsilon_{v,oc} \sum x_{oc}^{2} - \sum x_{oc} \sum \varepsilon_{v,oc} x_{oc}}{n \sum x_{oc}^{2} - \left[\sum x_{oc}\right]^{2}}$$
 Equation 7

where

$$x_{oc} = \ln \left( p_{oc} + c \cot \varphi' \right)$$
 Equation 8

and

$$\kappa^* = \frac{n\sum \varepsilon_{v,ur} x_{ur} - \sum \varepsilon_{v,ur} \sum x_{ur}}{n\sum x_{ur}^2 - \left[\sum x_{ur}\right]^2}$$
 Equation 9

$$\varepsilon_{v,ur}^{0} = \frac{\sum \varepsilon_{v,ur} \sum x_{ur}^{2} - \sum x_{ur} \sum \varepsilon_{v,ur} x_{ur}}{n \sum x_{ur}^{2} - \left[\sum x_{ur}\right]^{2}}$$
 Equation 10



where

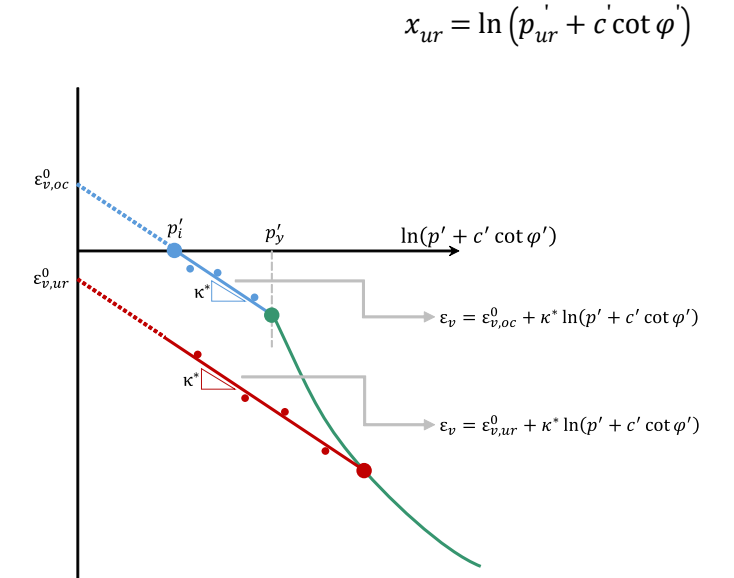


Figure 7. Determining the slope  $\kappa^*$  . Step 4

The fourth step is to determine the slope of the normal compression line  $\lambda^*$  (Figure 8). It should be noted that  $\lambda^*$  is the slope of the normal consolidation line in an isotropic loading condition. For other loading conditions, however, the normal consolidation branch is not necessarily linear, so the slope of its curve is not equal to  $\lambda^*$ . Based on the Soft Soil model's framework, that is a reformulated version of the Modify Cam Clay framework, it can be proven that there is another alternative space in which the sample response is linear even in a normal consolidation branch. The x and y axes in this space are functions of the measured parameters  $\varepsilon_v$ , p' and q, constants estimated in the previous steps (i.e.,  $\varphi$ , r and r), and the ellipse aspect ratio r.

$$x = \ln \left[ (p' + c'\cot \varphi')(M^2 + \eta^2) \right]$$
 Equation 12  

$$y = \varepsilon_v - \kappa^* \ln (p' + c'\cot \varphi')$$
 Equation 13

Where the stress ratio  $\eta$  is defined as:

$$\eta = \frac{q}{p + c \cot \varphi}$$
 Equation 14

The overconsolidation and unloading-reloading branches are both horizontal in this new space. The normal consolidation branch is a straight line. The slope of this line represents the difference between the isotropic normal consolidation slope  $\lambda^*$  and the over consolidation slope  $\kappa^*$ . Given that the constant  $\kappa^*$  is already estimated in the previous step, the constant  $\lambda^*$  can be found by applying the method of least squares on the proposed space:



**Equation 11** 

$$\lambda^* = \kappa^* + \frac{n\sum x_i y_i - \sum y_i \sum x_i}{n\sum x_i^2 - \left|\sum x_i\right|^2}$$
 Equation 15

According to Equation 12, the value of the ellipse aspect ratio M is required to determine the isotropic normal consolidation slope  $\lambda^*$ . This aspect ratio, however, is affected by the value of  $\lambda^*$  as follows:

$$M^{2} = \left[\frac{3(1 - K_{0}^{NC})}{1 + 2K_{0}^{NC}}\right]^{2} + \frac{3(\lambda^{*} - \kappa^{*})}{\frac{1 + 2K_{0}^{NC}}{3(1 - K_{0}^{NC})}} \lambda^{*} - \frac{1 + \mu_{s}}{3(1 - 2\mu_{s})} \kappa^{*}$$
Equation 16

Therefore, calculating the values of  $\lambda^*$  and M requires an iteration process. This process includes:

- 1. To guess a value for  $\lambda^*$ ,
- 2. To calculate the corresponding aspect ratio M using Equation 16,
- 3. To calculate a new value for  $\lambda^*$  using Equation 15 and Figure 8, and
- 4. To update the value of  $\lambda^*$  and to repeat the procedure from the stage 1.

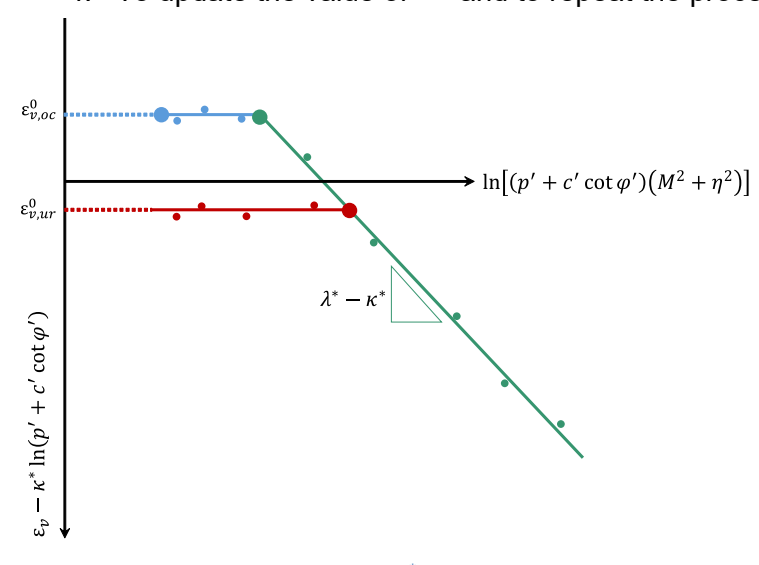


Figure 8. Determining the slope  $\lambda^*$ . Step 5

The fifth step is to determine the over-consolidation ratio  ${\cal OCR}$  for each specimen (Figure 9). This requires identification of the mean effective pressure p'y (see Figure 2) at which the response transitions from elastic to elastic-plastic; that is, from overconsolidated to normally compressed. More specifically, the  ${\cal OCR}$  is the ratio between the isotropic pre-consolidation pressure p'y and the isotropic initial pressure p'y. As stated earlier, the response of the sample changes from elastic to elastic-plastic only if a stress path engages the yield surface. As a result, for a stress path that is not necessarily isotropic, the yield pressure p'y is less than the isotropic pre-consolidation pressure, p'y. These two pressures, however, are not independent.

For example, in a drained triaxial test with a stress path of 3:1, the deviatoric stress at the yield surface is three times the difference between the yield and the initial pressures (Equation 17). The isotropic pre-consolidation pressure, p'v, can be expressed in terms of yield stresses using the yield function of the elliptical surface (Equation 18). Finally, the OCR for each sample is estimated as a ratio between the isotropic pre-consolidation pressure, p'v and the isotropic initial pressure p'v (Equation 19).

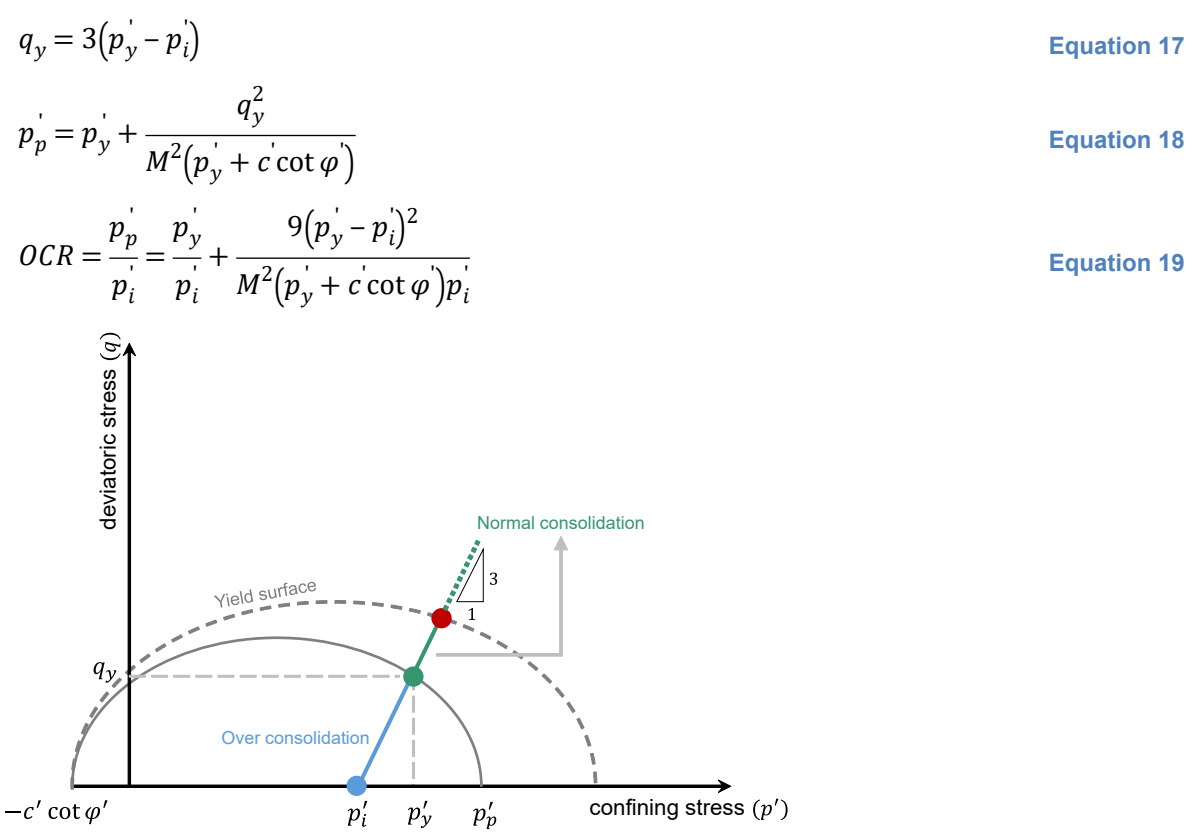


Figure 9. Determining the over-consolidation ratio OCR.

# **Application**

Figure 10 to Figure 14 summarize the parameterization procedure as applied to the results of three (A1, A2, and A3) drained triaxial tests on the Bothkennar clay (McGinty, 2006). Table 2 provides a summary of the model constants obtained from the parameterization procedure.

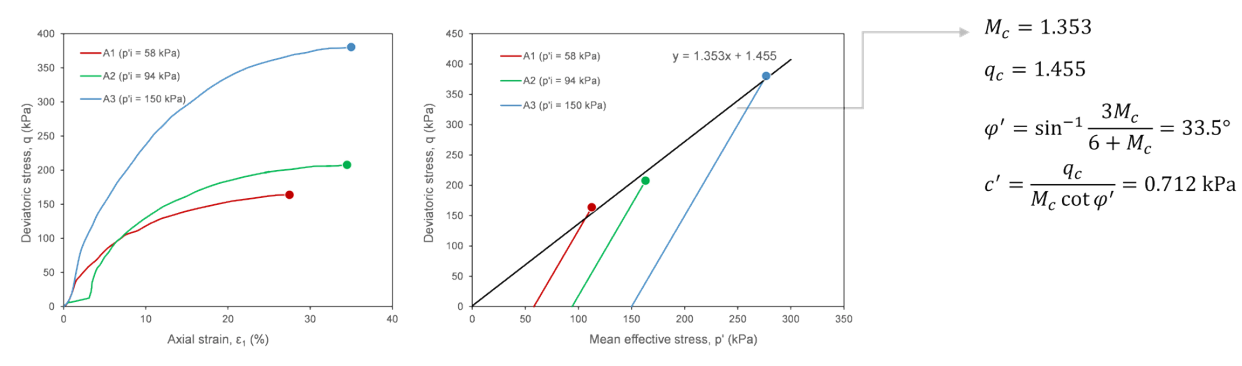


Figure 10. Step 1: determination of the strength properties.



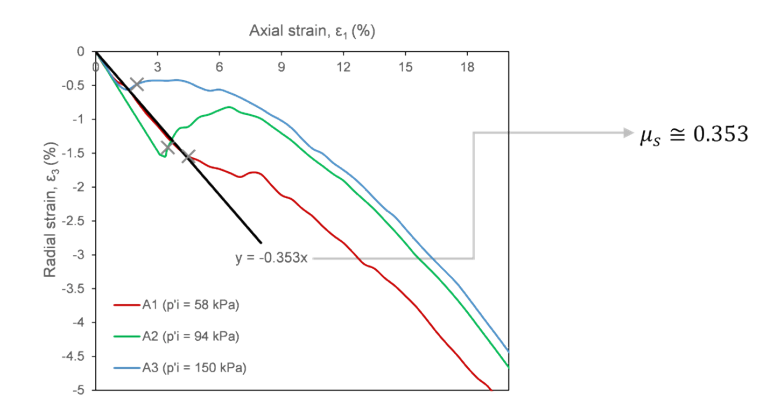


Figure 11. Step 2: determination of Poisson's ratio ( $\mu_s$ ).

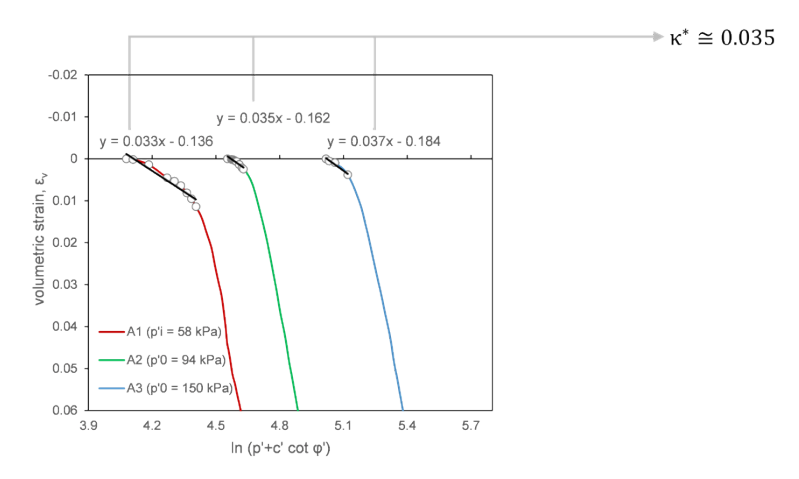


Figure 12. Step 3: determination of the slope  $\kappa^*$  .

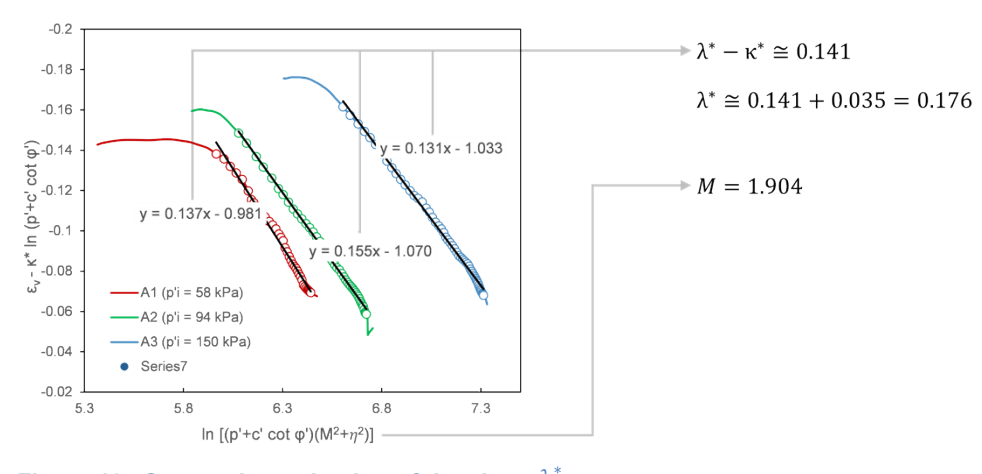
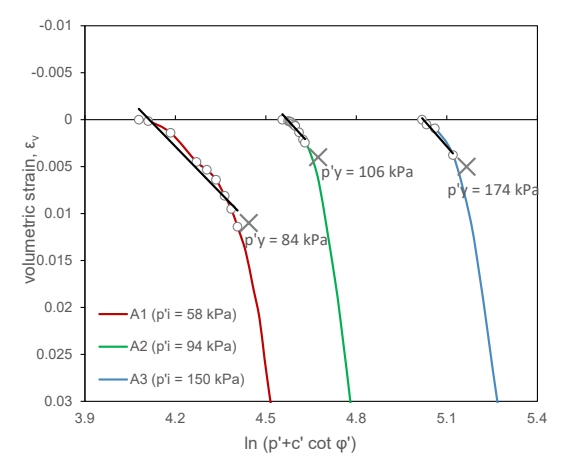


Figure 13. Step 4: determination of the slope  $\lambda^*$ .





$$p'_{p,A1} = 103.74 \text{ kPa}$$
  $OCR_{A1} = \frac{103.74}{58} = 1.789$   $p'_{p,A2} = 109.34 \text{ kPa}$   $OCR_{A2} = \frac{109.34}{94} = 1.163$   $p'_{p,A3} = 182.17 \text{ kPa}$   $OCR_{A3} = \frac{182.17}{150} = 1.214$ 

Figure 14. Step 5: determination of the overconsolidation ratio (OCR).



Table 2. Bothkennar clay model constants for the Soft Soil model

Parameter	Symbol	
Effective angle of shear resistance	$arphi^{'}$	33.5°
Effective cohesion	c <sup>'</sup>	0.712 kPa
Slope of normal compression line	λ*	0.176
Slope of the unloading-reloading line	κ*	0.035
Poisson's ratio	$\mu_{s}$	0.353
Over consolidation ratio (A1, A2, A3)	OCR	1.789; 1.163; 1.214
Initial void ratio (A1, A2, A3)	е	1.515; 1.447; 1.310

### Verification

Figure 15 through Figure 17 compare the measured, simulated, and analytical results for tests A1, A2, and A3. Discrete scatter points are laboratory results and continuous black lines are the results of the SIGMA/W simulations. The analytical results of the Soft Soil model are also shown in these diagrams as orange dashed lines. Refer to the associated GeoStudio project file to explore the analysis definitions and simulated results in detail.

The full compatibility of analytical and numerical curves shows the reliability of the model's implementation in SIGMA/W. In addition, the acceptable consistency between the laboratory results and simulations indicates the capabilities of the calibrated Soft Soil model in predicting the responses of the clay samples. The parameterization procedure relies on linear regression; consequently, the simulated/analytical results will generally provide a better fit to those specimens with measured data that was nearest the trend lines.

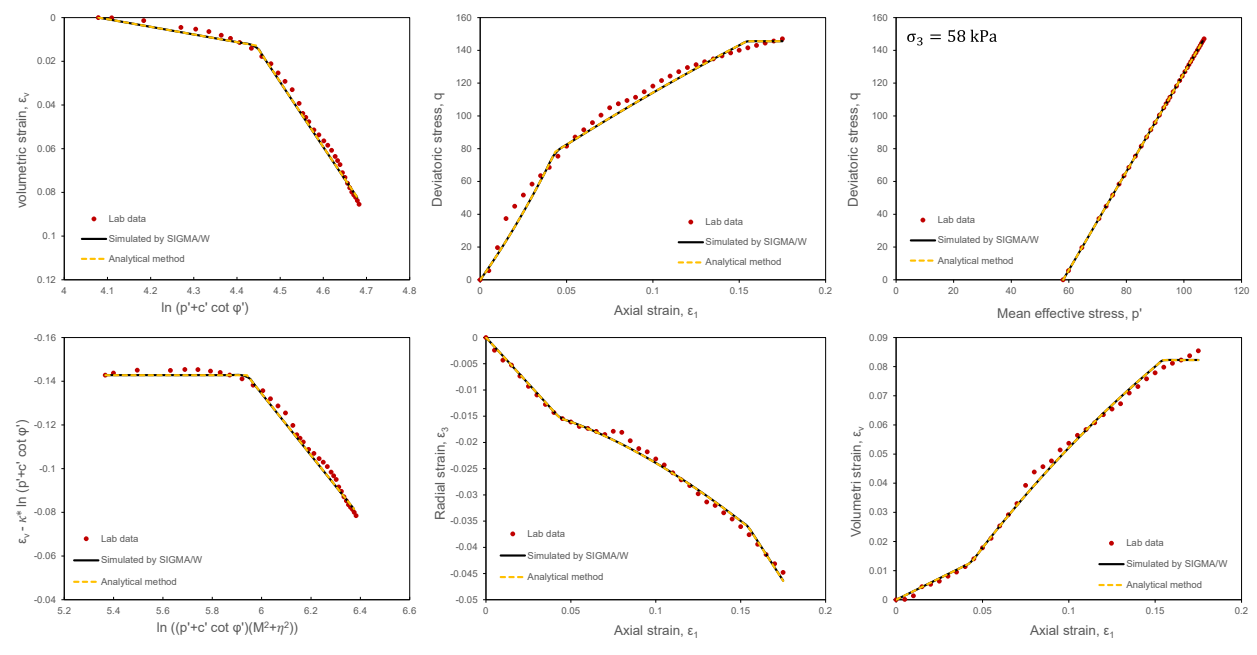


Figure 15. Comparison of simulated, analytical, and measured results for specimen A1.



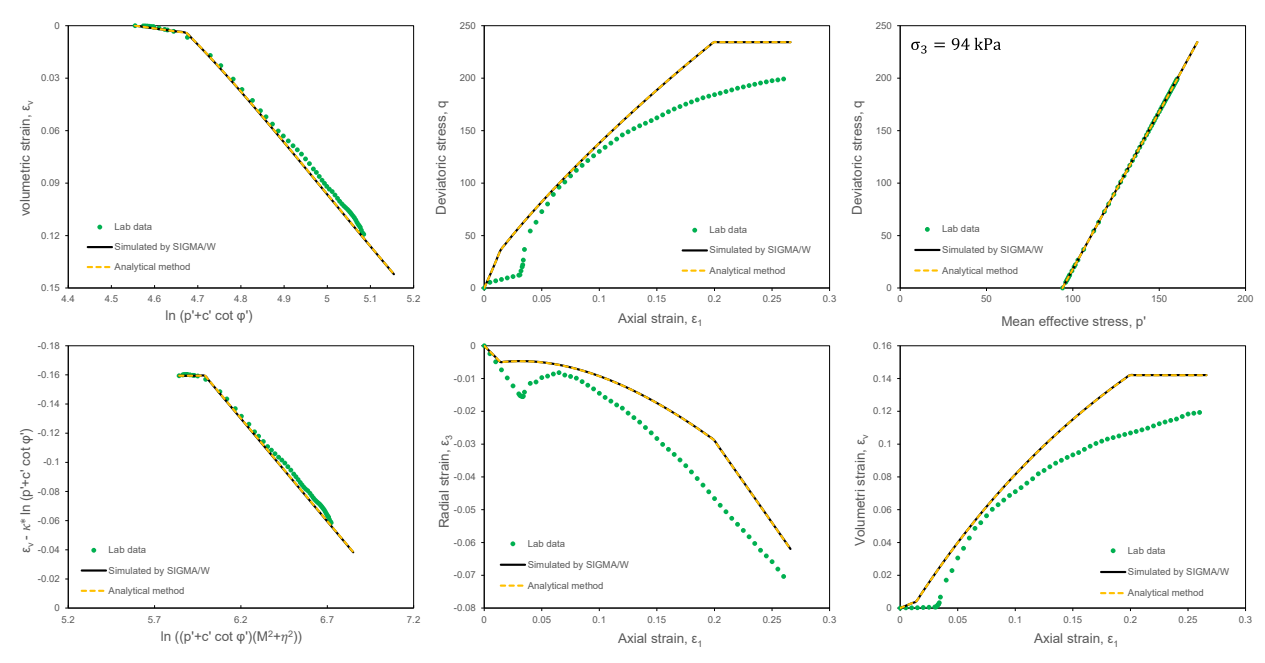


Figure 16. Comparison of simulated, analytical, and measured results for specimen A2.

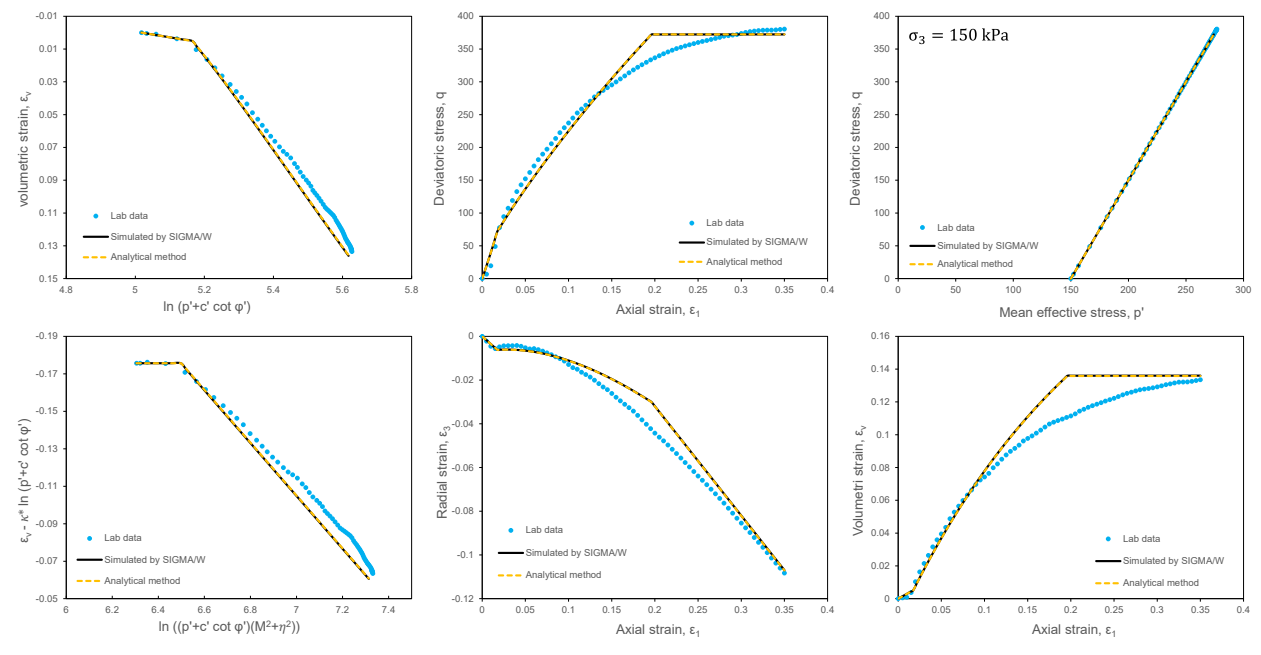


Figure 17. Comparison of simulated, analytical, and measured results for specimen A3.

# **Summary**

The calibration procedure of the Soft Soil model was provided in five straight forward steps. The results of the drained triaxial tests showed to be the only laboratory dataset required for parameterizing the model. The material constants were used in numerical simulations and the results were found to compare favorably with both the analytical solution and corresponding laboratory results.



# References

McGinty, K., 2006. The stress-strain behaviour of Bothkennar clay, Doctoral dissertation, University of Glasgow.

PLAXIS Material Models Manual. Connect Edition V21.01, 2021. Bentley.

Seequent ULC. 2024. Stress-strain modeling with GeoStudio. Calgary, Alberta, Canada.

